Y. H. Bian, Z. G. Tian

NONLINEAR THEORY OF THERMOMAGNETOELASTICITY OF SPHERICAL SEGMENT SHELLS WITH JOULE'S HEAT TAKEN INTO ACCOUNT

Key Laboratory of Mechanical Reliability for Heavy Equipments and Large Structures of Hebei Province, College of Civil Engineering and Mechanics, Yanshan University, Qinhuangdao, China; e-mail: byh0ysu@outlook.com

Abstract. A thermo-magneto-elastic problem for thin conductive spherical segment shells in a magnetic field is studied. The nonlinear magnetoelastic kinetic equations, electrodynamics equations, geometric equations, physical equations, and expressions for the Lorentz force of thin spherical segment shells under the action of electromagnetic field, temperature field, and mechanical field are given. The standard Cauchy form of nonlinear differential equations, which include eight basic unknowns in total, are obtained by the variable replacement method. Using Newmark's stable finite formulas and the quasi-linearization method, the nonlinear partial differential equations are transformed into a sequence of quasilinear differential equations, which can be solved by the discrete-orthogonalization method. A temperature field in the thin spherical segment shells and the integral eigenvalues of the temperature field are derived after considering Joule's heat effect in an electromagnetic field and the thermal equilibrium equation. The change rules of stresses, temperatures, and deformations in thin spherical segment shells with electromagnetic parameters are discussed. The results show that the stresses, strains, and temperatures can be controlled by adjusting the electromagnetic and mechanical parameters. The results presented here are expected to be a theoretical reference for the thermo-magneto-elastic analysis of thin conductive shells.

Keywords: magnetoelasticity of thin spherical segment shell, magnetic field, Lorentz force, nonlinearity, Joule heat.

1. Introduction.

Thermo-magneto-elastic theory is specially used to study the coupling effect of the electromagnetic field, the temperature field, and the deformation field. In modern industrial engineering, there are often some structural components of thin shell that need to work in the coupling environment of the electromagnetic field, the temperature field, and the mechanical field. Therefore, it is very important to analyze the stress-strain state of it. The thermo-magnetic elasticity includes classic elastic theory, the heat conduction theory, and the electromagnetic field theory. On the basis of these theories, the problems on the interaction of the electromagnetic field, the temperature field, and the deformation field are further solved.

At present, abundant achievements are obtained in the studies of the magnetoelastic vibration problems, stability problems, and stress-strain problems of electromagnetic structures, such as Pao and Yeh [1] (1973); Ambartsumyan [2] (1977); Moon [3] (1984); Van de Ven [4] (1986); Ulitko, Mol'chenko, Kovalchuk [5] (1994); Mol'chenko, Grigorenko [6] (2010); Mol'chenko [7 – 13] (1989, 2014, 2016, 2018, 2019, 2020, 2021); Bian [14, 15] (2015, 2021); Zheng, Wang [16] (2003); Hasanyan, Librescu, Ambur [17] (2006); Gao, Xu [18] (2010); Kuang [19] (2014); Vinyas, Sagar, Kattimani [20] (2018); Bi, Wang, Deng, Wang [21] (2020), and others. These achievements laid a good foundation for studies of the electromagnetic elastic mechanics and its applications. However, these researches fasten mostly on the **c**oupling problems of electromagnetic fields and mechanical fields, researches on a thermo-magneto-elastic problem with considering temperature fields have rarely been seen. Therefore, researches on thermo-magneto-elastic problems for conductive plates and shells have recently become one of the most important topics.

Electromagnetic structures in the electromagnetic field environment often exhibit complex multi-field coupling effects. It belongs to a new problem in the research field of electromagnetic elastic mechanics. Based on the nonlinear magnetoelastic kinetic equations, electrodynamics equations, geometric equations, and physical equations under the coupling field, the thermo-magneto-elastic fundamental equations for a thin spherical segment shell under the interaction of an electromagnetic field, a temperature field, and a mechanical field are given. The temperature field in a thin spherical segment shell and the integral eigenvalues of the temperature field are derived after considering Joule's heat effect in an electromagnetic field and the thermal equilibrium equation. The stresses, displacements, and temperatures of the thin spherical segment shell in a magnetic field are computed. The effect of the side current, magnetic induction intensity, etc. on the stresses, displacements, and temperatures in the thin spherical segment shell is analyzed. This lays the analytical foundation for developing and popularizing practical application of the thermo-magneto-elastic problem for plates and shells.

2. Thermo-Magneto-Elastic Fundamental Equations of Thin Spherical Segment Shells.

A three-dimensional orthogonal curvilinear coordinate system φ, θ, n is established on a spherical segment under the interaction of mechanical loads and an electromagnetic field as shown in Fig. 1. Under the action of axisymmetric loads, it can be regarded axisymmetric problem. By satisfying the magnetoelastic suppositions of the thin shell [7] and using elastic mechanics theories, Ohm's law and Maxwell equations in electromagnetic basic theories, the fundamental equations for thin spherical segment shell can be derived as follows:

The magnetoelastic kinetic equations are

$$\frac{\partial (rN_\varphi)}{\partial \varphi} - \frac{\partial r}{\partial \varphi} N_\theta + rQ_\varphi + Rr(P_\varphi + \rho f_\varphi) = Rr\rho h \frac{\partial^2 u}{\partial t^2}; \tag{1}$$

$$\frac{\partial (rQ_\varphi)}{\partial \varphi} - r(N_\varphi + N_\theta) + Rr(P_n + \rho f_n) = Rr\rho h \frac{\partial^2 w}{\partial t^2}; \tag{2}$$

$$\frac{\partial (rM_\varphi)}{\partial \varphi} - R\cos\varphi M_\theta - Rr\left(N_\varphi - \frac{M_\theta}{R}\right)\theta_\varphi - RrQ_\varphi = \frac{1}{12} Rr\rho h^3 \frac{\partial^2 \theta_\varphi}{\partial t^2}. \tag{3}$$

The electrodynamics equations are

$$-\frac{\partial B_n}{\partial t} = \frac{1}{Rr} \frac{\partial (rE_\theta)}{\partial \varphi}; \tag{4}$$

$$\sigma\mu\left[E_\theta + \frac{1}{2}\frac{\partial w}{\partial t}(B_\varphi^+ + B_\varphi^-) - \frac{\partial u}{\partial t} B_n\right] = -\frac{1}{R}\frac{\partial B_n}{\partial \varphi} + \frac{B_\varphi^+ - B_\varphi^-}{rh}. \tag{5}$$

The geometric equations are

$$\varepsilon_\varphi = \frac{1}{R}\frac{\partial u}{\partial \varphi} + \frac{w}{R} + \frac{1}{2}\theta_\varphi^2; \quad \varepsilon_\theta = \frac{u}{Rr}\frac{\partial r}{\partial \varphi} + \frac{w}{R}; \tag{6a, b}$$

$$\kappa_\varphi = \frac{1}{R}\frac{\partial \theta_\varphi}{\partial \varphi}; \quad \kappa_\theta = \frac{\theta_\varphi}{Rr}\frac{\partial r}{\partial \varphi}; \quad \theta_\varphi = -\frac{1}{R}\frac{\partial w}{\partial \varphi} + \frac{u}{R}. \tag{7a, b, c}$$

The physical equations are

$$N_{\varphi} = D_N [\varepsilon_{\varphi} + \nu\varepsilon_{\theta} - (1+\nu)\varepsilon_T]; \quad N_{\theta} = D_N [\varepsilon_{\theta} + \nu\varepsilon_{\varphi} - (1+\nu)\varepsilon_T]; \tag{8a, b}$$

$$M_{\varphi} = D_M [\kappa_{\varphi} + \nu\kappa_{\theta} - (1+\nu)\kappa_T]; \quad M_{\theta} = D_M [\kappa_{\theta} + \nu\kappa_{\varphi} - (1+\nu)\kappa_T], \tag{9a, b}$$

where σ is the electrical conductivity; μ is the permeability; ρ is the mass density; h is the shell thickness; R is the radius of the spherical segment; r is the radius of the section round; B_{φ}^{+} and B_{φ}^{-} are the values of B_{φ} on the inner and outer surfaces of the shell, respectively; ε_{φ} and ε_{θ} are the strains in the corresponding directions; κ_{φ} and κ_{θ} are the bending strains in the corresponding directions; u, w, and θ_{φ} are the displacements and rotation angle in the corresponding directions; E_{θ} is the electric field intensity in the θ-direction; B_n is the magnetic induction intensity in the n-direction; P_{φ} and P_n are the surface forces in the corresponding directions on the shell; ρf_{φ} and ρf_n are the Lorentz forces in the corresponding directions; N_{φ}, N_{θ}, Q_{φ}, M_{φ}, and M_{θ} are the internal forces and moments in the corresponding directions; $(D_N = Eh/(1-\nu^2))$ and $(D_M = Eh^3/[12(1-\nu^2)])$ are the tensile and bending rigidities of the shell, respectively; E is elastic modulus; ν is Poisson's ratio; ε_T and κ_T are the integral eigenvalues of the temperature field T along the thickness of the spherical segment, the γ-coordinate along the thickness is established at the neutral layer of the shell as shown in Fig. 1, we obtain:

$$\varepsilon_T = \frac{1}{h}\int_{-h/2}^{h/2} \alpha_T T(\varphi, \theta, n) d\gamma; \quad \kappa_T = \frac{12}{h^3}\int_{-h/2}^{h/2} \alpha_T T(\varphi, \theta, n)\gamma d\gamma, \tag{10a, b}$$

where α_T is the linear expansion coefficient of the material; $T(\varphi, \theta, n)$ is the temperature distributing function in the shell.

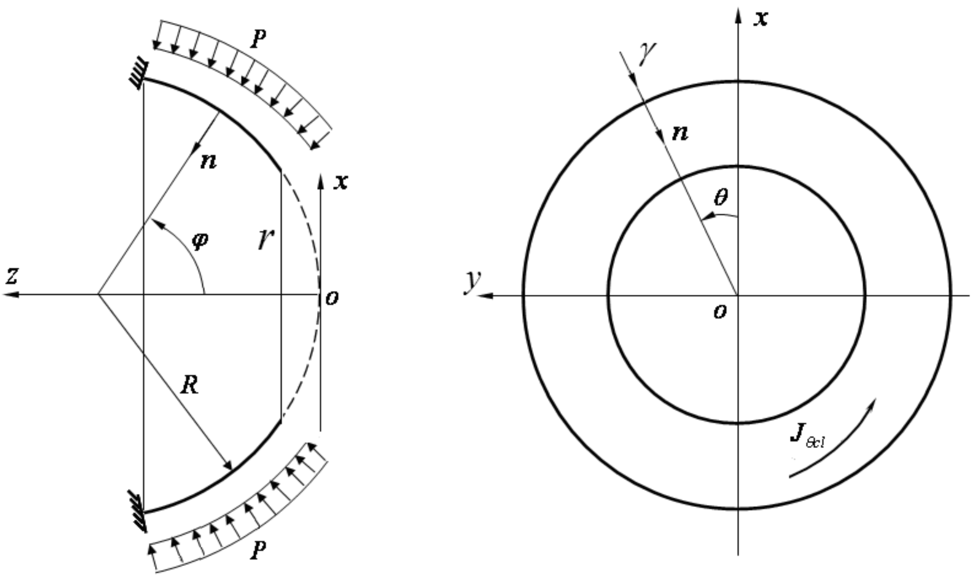

Fig. 1. A thin spherical segment shell in a magnetic field.

In order to obtain standard Cauchy form of nonlinear partial differential equations, we choose u, w, θ_φ, N_φ, Q_φ, M_φ, B_n and E_θ as the basic unknowns. The thermo-magneto-elastic fundamental equations for the spherical segment are obtained as

$$\frac{\partial u}{\partial \varphi}=\frac{R(1-\nu^2)}{Eh}N_\varphi-(1+\nu)\,w-\frac{\nu}{\tan\varphi}u-\frac{R}{2}\theta_\varphi^2+R(1+\nu)\varepsilon_T; \tag{11}$$

$$\frac{\partial w}{\partial \varphi}=-R\,\theta_\varphi+u; \tag{12}$$

$$\frac{\partial \theta_\varphi}{\partial \varphi}=\frac{12R(1-\nu^2)}{E h^3}M_\varphi-\frac{\nu}{\tan\varphi}\theta_\varphi+R(1+\nu)\kappa_T; \tag{13}$$

$$\frac{\partial N_\varphi}{\partial \varphi}=\frac{1}{\tan\varphi}\left[(\nu-1)N_\varphi+\frac{E h}{R}\left(\frac{u}{\tan\varphi}+w-R\varepsilon_T\right)\right]-Q_\varphi-R(P_\varphi+\rho f_\varphi)+R\rho h\frac{\partial^2 u}{\partial t^2}; \tag{14}$$

$$\frac{\partial Q_\varphi}{\partial \varphi}=-\frac{1}{\tan\varphi}Q_\varphi+(1+\nu)N_\varphi+\frac{Eh}{R}\left(\frac{u}{\tan\varphi}+w-R\varepsilon_T\right)-R(P_n+\rho f_n)+R\rho h\frac{\partial^2 w}{\partial t^2}; \tag{15}$$

$$\frac{\partial M_\varphi}{\partial \varphi}=\frac{1}{\tan\varphi}\left[(\nu-1)M_\varphi+\frac{E h^3}{12}\left(\frac{\theta_\varphi}{R\tan\varphi}-\kappa_T\right)\right]-\frac{E h^3}{12}\left(\frac{\theta\varphi}{R\tan\varphi}-\kappa_T\right)\theta_\varphi+$$

$$+R N_\varphi\theta_\varphi-\nu M_\varphi\theta_\varphi+R Q_\varphi+\frac{R\rho h^3}{12}\frac{\partial^2\theta_\varphi}{\partial t^2}; \tag{16}$$

$$\frac{\partial B_n}{\partial \varphi}=-R\sigma\mu\left[E_\theta+\frac{1}{2}(B_\varphi^+ + B_\varphi^-)\frac{\partial w}{\partial t}-B_n\frac{\partial u}{\partial t}\right]+\frac{(B_\varphi^+ - B_\varphi^-)}{h\sin\varphi}; \tag{17}$$

$$\frac{\partial E_\theta}{\partial \varphi}=-R\frac{\partial B_n}{\partial t}-\frac{1}{\tan\varphi}E_\theta. \tag{18}$$

3. Method for Solving the Thermo-Magneto-Elastic Problem for Thin Spherical Segment Shells.

Equations (11) − (18) can be written as the following boundary-value problems:

$$\frac{\partial \boldsymbol{N}}{\partial \varphi}=\boldsymbol{F}(\varphi,\boldsymbol{N})\quad(\varphi_0\le\varphi\le\varphi_n); \tag{19}$$

$$D_1\boldsymbol{N}(\varphi_0)=\boldsymbol{d}_1;\quad D_2\boldsymbol{N}(\varphi_n)=\boldsymbol{d}_2, \tag{20a, b}$$

where $\boldsymbol{N}=\{u, w, \theta_\varphi, N_\varphi, Q_\varphi, M_\varphi, B_n, E_\theta\}^{\mathrm{T}}$ is eight-dimensional vector; D_1 and D_2 are given orthogonal matrixes; $\boldsymbol{d}_1$ and $\boldsymbol{d}_2$ are given vectors.

Eq. (19) is a set of nonlinear partial differential equations with eight basic unknowns. The difficulties are how to solve directly the equations. First, Newmark's stable finite equi-different formulas [7] are used to find the derivatives with respect to time in Eqs. (11) − (18) according to the time step:

$$\ddot{N}^{t+\Delta t} = \frac{N^{t+\Delta t} - N^t}{\beta(\Delta t)^2} - \left[\frac{\dot{N}^t}{\Delta t} + \ddot{N}^t\left(\frac{1}{2} - \beta\right)\right]\frac{1}{\beta}; \quad \dot{N}^{t+\Delta t} = \dot{N}^t + \frac{\Delta t}{2}(\ddot{N}^t + \ddot{N}^{t+\Delta t}), \qquad (21a, b)$$

where Δt is the integration step; β is the parameter of the scheme. We choose $\beta = 0,25$.

After difference, Eqs. (11) – (18) can be expressed as

$$\frac{\mathrm{d}\boldsymbol{N}}{\mathrm{d}\varphi} = \boldsymbol{F}(\varphi, \boldsymbol{N}) \quad (\varphi_0 \le \varphi \le \varphi_n); \qquad (22)$$

$$D_1\boldsymbol{N}(\varphi_0) = \boldsymbol{d}_1; \quad D_2\boldsymbol{N}(\varphi_n) = \boldsymbol{d}_2. \qquad (23a, b)$$

The problems described in Eq. (22) are nonlinear. Using an iterative method, nonlinear problems can be transformed into a series of linear problems. Taken iterative equations are [7]

$$\frac{\mathrm{d}\boldsymbol{N}^{(k+1)}}{\mathrm{d}\varphi} = \boldsymbol{F}(\varphi, \boldsymbol{N}^{(k)}) + \boldsymbol{\Gamma}(\varphi, \boldsymbol{N}^{(k)})(\boldsymbol{N}^{(k+1)} - \boldsymbol{N}^{(k)}); \qquad (24)$$

$$D_1\boldsymbol{N}^{(k+1)}(\varphi_0) = \boldsymbol{d}_1; \quad D_2\boldsymbol{N}^{(k+1)}(\varphi_n) = \boldsymbol{d}_2 \quad (k = 0, 1, 2 \cdots), \qquad (25a, b)$$

where $\boldsymbol{\Gamma}(\varphi, \boldsymbol{N}^{(k)})$ is Jacobi's matrix.

Thus, Eqs. (11) – (18) can be written finally as

$$\frac{\mathrm{d}u^{(k+1)}}{\mathrm{d}\varphi} = \frac{R(1-\nu^2)}{Eh}N_\varphi^{(k+1)} - (1+\nu)w^{(k+1)} - \\ -\frac{\nu}{\tan\varphi}u^{(k+1)} + \frac{R}{2}(\theta_\varphi^{(k)})^2 - R\theta_\varphi^{(k+1)}\theta_\varphi^{(k)} + R(1+\nu)\varepsilon_T^{(k+1)}; \qquad (26)$$

$$\frac{\mathrm{d}w^{(k+1)}}{\mathrm{d}\varphi} = -R\theta_\varphi^{(k+1)} + u^{(k+1)}; \qquad (27)$$

$$\frac{\mathrm{d}\theta_\varphi^{(k+1)}}{\mathrm{d}\varphi} = \frac{12R(1-\nu^2)}{Eh^3}M_\varphi^{(k+1)} - \frac{\nu}{\tan\varphi}\theta_\varphi^{(k+1)} + R(1+\nu)\kappa_T^{(k+1)}; \qquad (28)$$

$$\frac{\mathrm{d}N_\varphi^{(k+1)}}{\mathrm{d}\varphi} = \frac{1}{\tan\varphi}\left[(\nu-1)N_\varphi^{(k+1)} - Eh\varepsilon_T^{(k+1)} + \frac{Eh}{R}\left(\frac{1}{\tan\varphi}u^{(k+1)} + w^{(k+1)}\right)\right] - Q_\varphi^{(k+1)} - \\ -R(P_\varphi + \rho f_\varphi)^{(k+1)} + R\rho h\frac{\partial^2 u^{(k+1)}}{\partial t^2}; \qquad (29)$$

$$\frac{\mathrm{d}Q_\varphi^{(k+1)}}{\mathrm{d}\varphi} = -\frac{1}{\tan\varphi}Q_\varphi^{(k+1)} + (1+\nu)N_\varphi^{(k+1)} - Eh\varepsilon_T^{(k+1)} + \frac{Eh}{R}\left(\frac{1}{\tan\varphi}u^{(k+1)} + w^{(k+1)}\right) - \\ -R(P_n + \rho f_n)^{(k+1)} + R\rho h\frac{\partial^2 w^{(k+1)}}{\partial t^2}; \qquad (30)$$

$$\frac{\mathrm{d}\,M_{\varphi}^{(k+1)}}{\mathrm{d}\varphi}=\frac{1}{\tan\varphi}\left[(\nu-1)\,M_{\varphi}^{(k+1)}+\frac{Eh^3}{12}\left(\frac{1}{R\tan\varphi}\,\theta_{\varphi}^{(k+1)}-\kappa_T^{(k+1)}\right)\right]+$$

$$+R\left[N_{\varphi}^{(k+1)}\theta_{\varphi}^{(k)}+N_{\varphi}^{(k)}\theta_{\varphi}^{(k+1)}-N_{\varphi}^{(k)}\theta_{\varphi}^{(k)}\right]-$$

$$-\nu\left[M_{\varphi}^{(k+1)}\theta_{\varphi}^{(k)}+M_{\varphi}^{(k)}\theta_{\varphi}^{(k+1)}-M_{\varphi}^{(k)}\theta_{\varphi}^{(k)}\right]-\frac{Eh^3}{12R\tan\varphi}\left[2\theta_{\varphi}^{(k+1)}\theta_{\varphi}^{(k)}-(\theta_{\varphi}^{(k)})^2\right]+ \tag{31}$$

$$+\frac{Eh^3}{12}\left[\kappa_T^{(k+1)}\theta_{\varphi}^{(k)}+\kappa_T^{(k)}\theta_{\varphi}^{(k+1)}-\kappa_T^{(k)}\theta\varphi_{\varphi}^{(k)}\right]+R\,Q_{\varphi}^{(k+1)}+\frac{R\rho h^3}{12}\frac{\partial^2\theta\varphi_{\varphi}^{(k+1)}}{\partial t^2};$$

$$\frac{\mathrm{d}\,B_n^{(k+1)}}{\mathrm{d}\varphi}=$$

$$=-R\sigma\mu\left[E_{\theta}^{(k+1)}+\frac{1}{2}(B_{\varphi}^{+}+B_{\varphi}^{-})\frac{\partial\,w^{(k+1)}}{\partial\,t}-B_n^{(k)}\frac{\partial\,u^{(k+1)}}{\partial\,t}-B_n^{(k+1)}\frac{\partial\,u^{(k)}}{\partial\,t}+B_n^{(k)}\frac{\partial\,u^{(k)}}{\partial\,t}\right]+ \tag{32}$$

$$+\frac{(B_{\varphi}^{+}-B_{\varphi}^{-})}{h\sin\varphi};$$

$$\frac{\mathrm{d}\,E_{\theta}^{(k+1)}}{\mathrm{d}\varphi}=-R\,\frac{\partial B_n^{(k+1)}}{\partial\,t}-\frac{1}{\tan\varphi}\,E_{\theta}^{(k+1)}. \tag{33}$$

The Lorentz forces in Eqs. (26) – (33) can be written as

$$\rho f_{\varphi}^{(k+1)}=hJ_{\theta cl}B_n^{(k+1)}+\sigma h\left(E_{\theta}^{(k+1)}B_n^{(k)}+E_{\theta}^{(k)}B_n^{(k+1)}-E_{\theta}^{(k)}B_n^{(k)}\right)+$$

$$+\frac{1}{2}\sigma h(B_{\varphi}^{+}+B_{\varphi}^{-})\left(B_n^{(k)}(\dot{w}^{t+\Delta t})^{(k+1)}+B_n^{(k+1)}(\dot{w}^{t+\Delta t})^{(k)}-B_n^{(k)}(\dot{w}^{t+\Delta t})^{(k)}\right)- \tag{34}$$

$$-\sigma h\left[(B_n^{(k)})^2(\dot{u}^{t+\Delta t})^{(k+1)}+2B_n^{(k)}B_n^{(k+1)}(\dot{u}^{t+\Delta t})^{(k)}-2(B_n^{(k)})^2(\dot{u}^{t+\Delta t})^{(k)}\right];$$

$$\rho f_n^{(k+1)}=-\frac{1}{2}h\,J_{\theta cl}(B_{\varphi}^{+}+B_{\varphi}^{-})-$$

$$-\sigma h\left\{\left[\frac{1}{12}(B_{\varphi}^{+}-B_{\varphi}^{-})^2+\frac{1}{4}(B_{\varphi}^{+}+B_{\varphi}^{-})^2\right](\dot{w}^{t+\Delta t})^{(k+1)}+\frac{1}{2}(B_{\varphi}^{+}+B_{\varphi}^{-})E_{\theta}^{(k+1)}-\right.$$

$$-\frac{1}{2}(B_{\varphi}^{+}+B_{\varphi}^{-})\left(B_n^{(k)}(\dot{u}^{t+\Delta t})^{(k+1)}+B_n^{(k+1)}(\dot{u}^{t+\Delta t})^{(k)}-B_n^{(k)}(\dot{u}^{t+\Delta t})^{(k)}\right)- \tag{35}$$

$$\left.-\frac{h}{12}(B_{\varphi}^{+}-B_{\varphi}^{-})\left(B_n^{(k)}(\dot{\theta}_{\varphi}^{t+\Delta t})^{(k+1)}+B_n^{(k+1)}(\dot{\theta}_{\varphi}^{t+\Delta t})^{(k)}-B_n^{(k)}(\dot{\theta}_{\varphi}^{t+\Delta t})^{(k)}\right)\right\};$$

4. Electromagnetic Temperature Effect.

By using the electrodynamics equations and generalized Ohm's law, and considering the side electric current $J_{\varphi cl}$ and $J_{\theta cl}$, we have [7]:

$$J_{\varphi}=J_{\varphi cl}+\sigma E_{\varphi}+\sigma\left(\frac{\partial v}{\partial t}B_n-\frac{\partial w}{\partial t}B_{\theta}\right);\quad J_{\theta}=J_{\theta cl}+\sigma E_{\theta}+\sigma\left(\frac{\partial\,w}{\partial\,t}B_{\varphi}-\frac{\partial\,u}{\partial\,t}B_n\right). \tag{36a, b}$$

Due to Joule's heat effect in the electromagnetic field, the heat source is bound to be generated in the spherical segment. So the heat source power can be expressed as [22]

$$Q = 0,86\frac{J^2}{\sigma} = 0,86\frac{J_\varphi^2 + J_\theta^2}{\sigma}. \tag{37}$$

Regardless of local temperature effect at the ends of the spherical segment and external heating source, considering only the heat exchange between the inner and outer surfaces of the spherical segment and the outside, we think that the distribution of the heat source power density along the direction of the shell thickness is uniform. At $\gamma = 0$, the heat flow density $q = 0$; at $\gamma = h/2$, the heat flow density $q = Qh/2$, and $T = T_w$.

Thus, the temperature curve equation along the γ-direction is

$$T = T_f + \frac{Qh^2}{8\lambda_T}\left[1 + \frac{4\lambda_T}{h\alpha_F} - 4\left(\frac{\gamma}{h}\right)^2\right] - \frac{\rho hc}{2\alpha_F}\dot{T}_w, \tag{38}$$

where λ_T is the heat exchange coefficient of the material; c is the specific heat capacity of the material; α_F is the surface heat exchange coefficient of the material; T_w is the surface temperature of the shell; T_f is the temperature of the medium bordering upon the shell; $\dot{T}_w$ is the change rate of the surface temperature.

By using Eqs. (10), (36), (37), and (38), we have:

$$\varepsilon_T^{(k+1)} =$$

$$= \frac{43\alpha_T h^2}{400\sigma\lambda_T}\left\{ J_{\theta cl}^2 + \sigma^2\left[2E_\theta^{(k+1)}E_\theta^{(k)} - (E_\theta^{(k)})^2\right] + \sigma^2\left[B_\varphi^2\left(2\frac{\partial w^{(k+1)}}{\partial t}\frac{\partial w^{(k)}}{\partial t} - \left(\frac{\partial w^{(k)}}{\partial t}\right)^2\right) + \right.\right.$$

$$+ 2\frac{\partial u^{(k+1)}}{\partial t}\frac{\partial u^{(k)}}{\partial t}(B_n^{(k)})^2 + 2\left(\frac{\partial u^{(k)}}{\partial t}\right)^2 B_n^{(k+1)}B_n^{(k)} - 3\left(\frac{\partial u^{(k)}}{\partial t}\right)^2 (B_n^{(k)})^2 -$$

$$\left. - 2B_\varphi\left(\frac{\partial w^{(k+1)}}{\partial t}\frac{\partial u^{(k)}}{\partial t}B_n^{(k)} + \frac{\partial w^{(k)}}{\partial t}\frac{\partial u^{(k+1)}}{\partial t}B_n^{(k)} + \frac{\partial w^{(k)}}{\partial t}\frac{\partial u^{(k)}}{\partial t}B_n^{(k+1)} - 2\frac{\partial w^{(k)}}{\partial t}\frac{\partial u^{(k)}}{\partial t}B_n^{(k)}\right)\right] +$$

$$+ 2J_{\theta cl}\sigma E_\theta^{(k+1)} + 2J_{\theta cl}\sigma\left(\frac{\partial w^{(k+1)}}{\partial t}B_\varphi - \frac{\partial u^{(k+1)}}{\partial t}B_n^{(k)} - \frac{\partial u^{(k)}}{\partial t}B_n^{(k+1)} + \frac{\partial u^{(k)}}{\partial t}B_n^{(k)}\right) +$$

$$+ 2\sigma^2\left[B_\varphi\left(E_\theta^{(k+1)}\frac{\partial w^{(k)}}{\partial t} + E_\theta^{(k)}\frac{\partial w^{(k+1)}}{\partial t} - E_\theta^{(k)}\frac{\partial w^{(k)}}{\partial t}\right) - \right.$$

$$\left.\left. - \left(E_\theta^{(k+1)}B_n^{(k)}\frac{\partial u^{(k)}}{\partial t} + E_\theta^{(k)}B_n^{(k+1)}\frac{\partial u^{(k)}}{\partial t} + E_\theta^{(k)}B_n^{(k)}\frac{\partial u^{(k+1)}}{\partial t} - 2E_\theta^{(k)}B_n^{(k)}\frac{\partial u^{(k)}}{\partial t}\right)\right]\right\} \times$$

$$\times\left(\frac{4\lambda_T}{h\alpha_F} + \frac{2}{3}\right) - \frac{\alpha_T\rho hc}{2\alpha_F}\frac{\partial T_w^{(k+1)}}{\partial t}; \tag{39}$$

$$\kappa_T^{(k+1)} = 0. \tag{40}$$

The $\varepsilon_T^{(k+1)}$ and $\kappa_T^{(k+1)}$ are substituted in Eqs. (26) – (33), the thermo-magneto-elastic coupling equations for the spherical segment are obtained. All unknowns can be found by the discrete-orthogonalization method.

5. Example and Analysis.

A thin spherical segment shell made from copper shown in figure 1 is in a magnetic field $\boldsymbol{B} = \{B_\varphi, 0, 0\}$. It bears the mechanical load $\boldsymbol{P} = \{0, 0, P_n\}$. The electric current density in the shell is $\boldsymbol{J_{cl}} = \{0, J_{\theta cl}, 0\}$. We know $E = 100\,\text{GPa}$; $\nu = 0{,}3$; $\rho = 8200\,\text{kg/m}^3$; $\sigma = 5{,}88\times10^7 (\Omega\cdot\text{m})^{-1}$; $\mu = 1{,}25\times10^{-6}\,\text{H/m}$; $\lambda_T = 401\,\text{W/(m}\cdot{}^\circ\text{C)}$; $\alpha_F = 400\,\text{W/(m}^2\cdot{}^\circ\text{C)}$; $\alpha_T = 1{,}65\times10^{-6}\,{}^\circ\text{C}^{-1}$; $J_{\theta cl} = J_\theta \sin\omega t\,\text{A/m}^2$; $\omega = \pi\times10^2\,\text{sec}^{-1}$; $P_n = 500\,\text{N/m}^2$; $h = 2\times10^{-3}\,\text{m}$; $R = 1\,\text{m}$; $\varphi_0 = \pi/6$; $\varphi_n = \pi/3$.

The boundary conditions are

$$\varphi = \varphi_0:\quad N_\varphi = 0;\quad Q_\varphi = 0;\quad M_\varphi = 0;\quad B_n = 0; \qquad (41\text{a–d})$$

$$\varphi = \varphi_n:\quad u = 0;\quad w = 0;\quad \theta_\varphi = 0;\quad B_n = 0{,}01\sin\omega t\,\text{T}. \qquad (42\text{a–d})$$

The initial conditions are

$$\boldsymbol{N}(\kappa, t)\big|_{t=0} = 0;\quad \dot{u}(\varphi, t)\big|_{t=0} = 0;\quad \dot{w}(\varphi, t)\big|_{t=0} = 0;\quad \dot{\theta}_\varphi(\varphi, t)\big|_{t=0} = 0. \qquad (43\text{a–d})$$

Programming Eqs. (26) – (33) and conducting computations for the known data and the boundary and initial conditions yield the eight basic unknowns u, w, θ_φ, N_φ, Q_φ, M_φ, B_n and E_θ. Then the relations and change rules between the mechanical and electromagnetic variables can be ascertained by changing the relevant parameters.

Fig. 2 gives the deflection distribution in the spherical segment shell in the φ-direction for $J_\theta = 1{,}5\,\text{MA/m}^2$; $B_\varphi = 0{,}01\,\text{T}$ and $t = 10\,\text{sec}$. According to Fig. 2, when the electric current density or magnetic induction intensity is relatively large, the effect of the temperature on structural deformation is remarkable. Fig. 3 gives the variation of the deflection at the free end $(\varphi = \varphi_0)$ with time for $J_\theta = 1{,}5\,\text{MA/m}^2$ and different magnetic induction intensity. According to Fig. 3, the effect of the magnetic induction intensity on the free end vibration is remarkable, the amplitude of the free end vibration increases with increase in the magnetic induction intensity. Fig. 4 gives the variation of the deflection at the free end $(\varphi = \varphi_0)$ with time for $B_\varphi = 0{,}01\,\text{T}$ and different electric current density. According to Fig. 4, the effect of the electric current density on the free end vibration is remarkable.

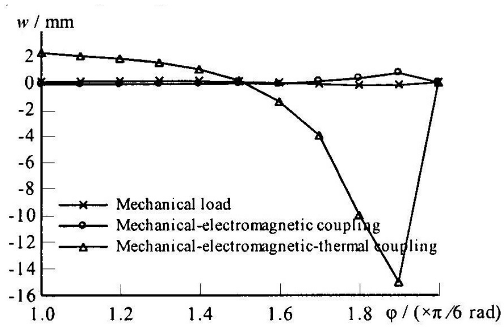

Fig. 2. Effects of the coupling action on the deflection in the spherical segment shell.

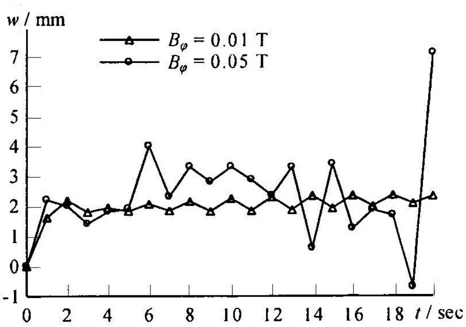

Fig. 3. The deflection at the free end versus t for $J_\theta = 1{,}5\,\text{MA}/\text{m}^2$ and different values of B_φ.

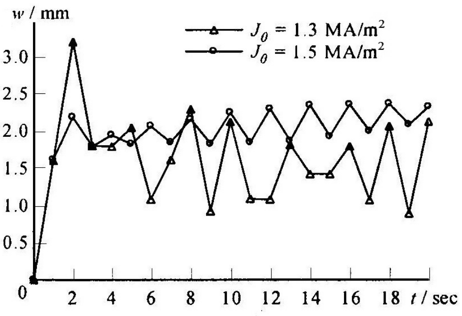

Fig. 4. The deflection at the free end versus t for $B_\varphi = 0{,}01\,\mathrm{T}$ and different values of J_θ.

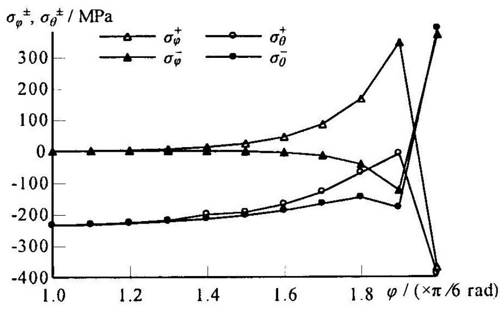

Fig. 5. Curves of the stress distribution for $J_\theta = 2{,}8\,\mathrm{MA/m^2}$, $B_\varphi = 0{,}01\,\mathrm{T}$, and $t = 10\,\mathrm{sec}$.

Fig. 5 gives the stress distribution in the φ-direction under the interaction of an electromagnetic field, a temperature field, and a mechanical field for $J_\theta = 2{,}8\,\mathrm{MA/m^2}$, $B_\varphi = 0{,}01\,\mathrm{T}$, and $t = 10\,\mathrm{sec}$. Curves σ_φ^+ and σ_φ^- are the normal stresses in the φ-direction on the inner, outer surfaces of the shell, respectively; curves σ_θ^+ and σ_θ^- are the normal stresses in the θ-direction on the inner, outer surfaces of the shell, respectively. Fig. 6 gives the variation of the stresses at the fixed end $(\varphi = \varphi_n)$ with time for $J_\theta = 1{,}5\,\mathrm{MA/m^2}$ and $B_\varphi = 0{,}01\,\mathrm{T}$. Curves σ_φ^+ and σ_φ^- are the variation of normal stresses in the φ-direction on the inner, outer surfaces of the shell with time, respectively; curves σ_θ^+ and σ_θ^- are the variation of normal stresses in the θ-direction on the inner, outer surfaces of the shell with time, respectively. According to Fig. 6, the absolute value of the stresses increases with increase in time. The stresses on the inner, outer surfaces of the shell are shown as the tensile and compressive stresses, but the absolute value is not exactly the same because of the effect of the axial forces. Fig. 7 gives the distribution of the Lorentz force ρf_φ and ρf_n in the spherical segment shell in the φ-direction for $J_\theta = 1{,}5\,\mathrm{MA/m^2}$, $B_\varphi = 0{,}01\,\mathrm{T}$, $t = 8\,\mathrm{sec}$, and $t = 10\,\mathrm{sec}$. According to Fig. 7, the absolute value of the ρf_φ is smaller than that of the ρf_n. The change of the ρf_φ is more obvious with increase in time, especially near the fixed end, this is reflected in the variation laws of the displacement or stress. As shown in Fig. 6, the absolute value of the stresses increases with increase in time, and the change of the stresses in the φ-direction is more remarkable than that of the stresses in the θ-direction.

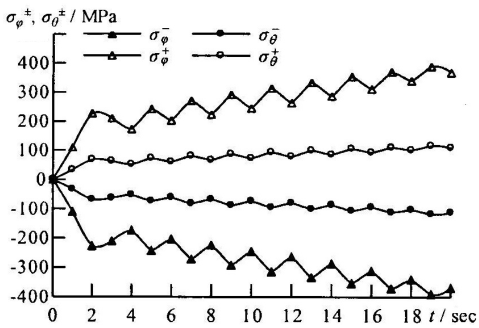

Fig. 6. The stress at the fixed end versus t for $J_\theta = 1{,}5\,\mathrm{MA/m^2}$ and $B_\varphi = 0{,}01\,\mathrm{T}$.

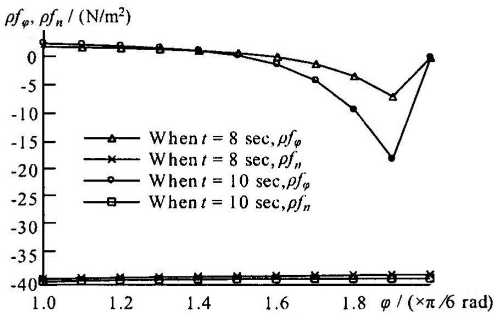

Fig. 7. Curves of the Lorentz force distribution for $J_\theta = 1{,}5\,\mathrm{MA/m^2}$ and $B_\varphi = 0{,}01\,\mathrm{T}$.

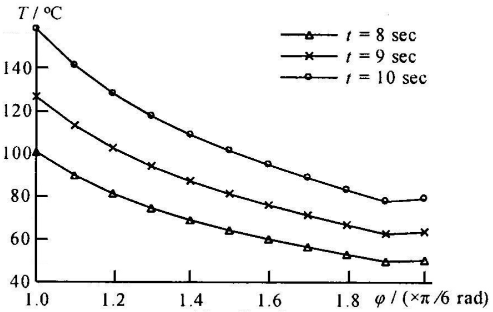

Fig. 8. Curves of the temperature distribution for $J_\theta = 1{,}5\,\mathrm{MA/m^2}$, $B_\varphi = 0{,}01\,\mathrm{T}$, and different moment.

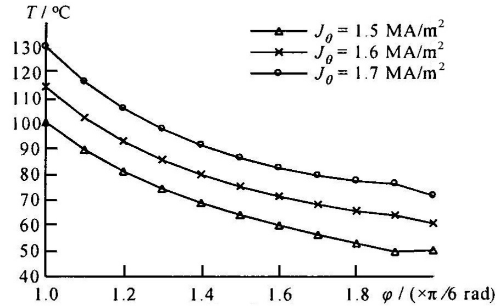

Fig. 9. Curves of the temperature distribution for $B_\varphi = 0{,}01\,\mathrm{T}$, $t = 8\,\mathrm{sec}$, , and different values of J_θ.

Fig. 8 gives the temperature distribution in the spherical segment shell in the φ-direction for $J_\theta = 1{,}5\,\mathrm{MA/m^2}$; $B_\varphi = 0{,}01\,\mathrm{T}$ and different moment. According to Fig. 8, the temperature in the shell decreases gradually from the free end to the fixed end, and the temperature increases with increase in time. Fig. 9 gives the temperature distribution in the spherical segment shell in the φ-direction for $B_\varphi = 0{,}01\,\mathrm{T}$, $t = 8\,\mathrm{sec}$, and different electric current density. According to Fig. 9, the temperature in the shell increases with increase in the electric current density. Fig. 10 gives the variation of the temperature at the fixed end $(\varphi = \varphi_n)$ with time for $B_\varphi = 0{,}01\,\mathrm{T}$ and different electric current density. According to Fig. 10, the temperature at the fixed end increases with increase in time.

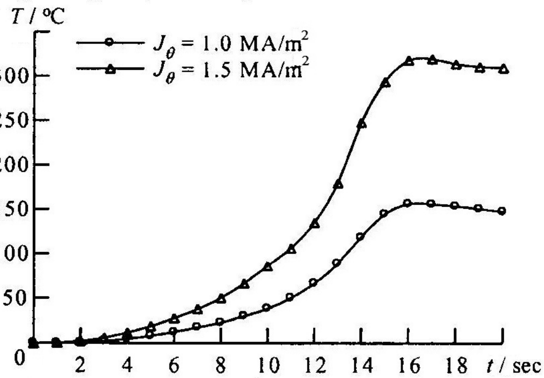

Fig. 10. The temperature at the fixed end versus t for $B_\varphi = 0{,}01\,\mathrm{T}$ and different values of J_θ.

6. Conclusions.

A thermo-magneto-elastic problem for a thin conductive spherical segment shell in a magnetic field has been studied. Based on fundamental equations of the mechanics, electrodynamics, and heat transfer theory, the fundamental equations for the thermo-magneto-elastic problem have been established. Using Newmark's stable finite equidifferent formulas and the quasi-linearization method, we have converted the nonlinear partial differential equations with eight basic unknowns into standard Cauchy form linear ordinary differential equations, which can be solved by the discrete-orthogonalization method. Numerical solutions for magnetoelastic stresses and deformations in a thin spherical segment shell under the interaction of an electromagnetic field, a temperature field, and a mechanical field have been obtained. By the results, we now know that:

(1) the influence of the electromagnetic field of low intensity on the temperature, deformation, and stress of structures is weak, this influence becoming stronger with the increase of electromagnetic field intensity; it is illustrated that the thermo-magneto-elastic analysis on structures in electromagnetic fields is necessary and very important;

(2) the deformations and stresses in a thin spherical segment shell show a nonlinear increasing trend with the electric current density or magnetic induction intensity;

(3) when the electric current density is high, the electromagnetic thermal effect can not be neglected. When the electric current density reaches a certain value, thermal stress will dominate;

(4) the stresses, strains, and temperatures in plates and shells can be controlled through adjusting the electromagnetic and mechanical parameters;

(5) the kinetic behavior of thin shells can be altered by changing the electric current density or magnetic induction intensity.

Acknowledgements.

This research was financially supported by the National Natural Science Foundation of China, the Foundation of Key Laboratory of Nonlinear Continuum Mechanics, Institute of Mechanics of Chinese Academy of Sciences. The authors gratefully acknowledge these supports.

РЕЗЮМЕ. Досліджено термомагнітопружну задачу для тонких провідних сферичних сегментних оболонок у магнітному полі. Наведено нелінійні магнітопружні кінетичні рівняння, рівняння електродинаміки, геометричні рівняння, фізичні рівняння та вирази для сили Лоренца тонких сферичних сегментних оболонок при взаємодії електромагнітного поля, поля температури та механічного поля. Методом заміни змінних отримано стандартну форму Коші нелінійних диференціальних рівнянь, які включають всього вісім основних невідомих. Використовуючи стійкі скінченні формули Ньюмарка та метод квазілінеаризації, ми перетворили нелінійні диференціальні рівняння в частинних похідних у послідовність квазілінійних диференціальних рівнянь, які можна розв'язати методом дискретної ортогоналізації. Температурне поле в тонких сферичних сегментних оболонках та інтегральні власні значення температурного поля виводяться після врахування теплового ефекту Джоуля в електромагнітному полі та рівняння теплової рівноваги. Обговорено закономірності зміни напружень, температур і деформацій в тонких сферичних сегментних оболонках з електромагнітними параметрами. Результати показують, що напруження, деформації та температури в пластинах і оболонках можна контролювати шляхом регулювання електромагнітних і механічних параметрів. Можна передбачити, що наведені результати будуть теоретичною базою для термомагнітопружного аналізу тонких провідних оболонок.

КЛЮЧЕВЫЕ СЛОВА: магнітопружність тонкої сферичної сегментної оболонки, магнітне поле, сила Лоренца, нелінійність, Джоулеве тепло.

1. *Y.H. Pao and C. S. Yeh.* "A linear theory for soft ferromagnetic elastic bodies," Int. J. Eng. Sci., **11**, No. 4, 415 – 436 (1973).
2. *S.A. Ambartsumyan, G.E. Bagdasaryan, and M.V. Belubekyan.* Magnetoelasticity of Thin Shells and Plates [in Russian], Nauka, Moscow (1977).
3. *F.C. Moon.* Magneto-Solid Mechanics. John Wiley & Sons, New York (1984).
4. *A.A.F. Van de Ven and M. J.H. Couwenberg.* "Magneto-elastic stability of a superconducting ring in its own field," J. Eng. Math., **20**, 251 – 270 (1986).
5. *A.T. Ulitko, L.V. Mol'chenko and V.F. Kovalchuk.* Magnetoelasticity under Dynamic Loading: A Workbook [in Ukrainian], Lybid', Kyiv (1994).
6. *L.V. Mol'chenko and Ya.M. Grigorenko.* Fundamental Theory of Magnetoelasticity for Elements of Thin Plates and Shells: A Textbook [in Ukrainian], Kyiv University (2010).
7. *L.V. Mol'chenko*. Nonlinear Magnetoelasticity of Thin Current-Carrying Shells [in Russian], Vyshcha Shkola, Kyiv (1989).
8. *L.V. Mol'chenko, I.I. Loos and L.N. Fedorchenko*. "Influence of extraneous current on the stress state of an orthotropic ring plate with orthotropic conductivity," Int. Appl. Mech., **50**, No. 6, 683 – 687 (2014).
9. *L.V. Mol'chenko, I.I. Loos and L.N. Fedorchenko*. "Deformation of a flexible orthotropic spherical shell of variable stiffness in a magnetic field," Int. Appl. Mech., **52**, No. 1, 56 – 61 (2016).

10. *L.V. Mol'chenko, L.N. Fedorchenko and L.Ya. Vasil'eva.* "Nonlinear theory of magnetoelasticity of shells of revolution with Joule heat taken into account," Int. Appl. Mech., **54**, No. 3, 306 – 314 (2018).
11. *L.V. Mol'chenko and I.I. Loos.* "Thermomagnetoelastic deformation of a flexible orthotropic conical shell with electrical conductivity and Joule heat taken into account," Int. Appl. Mech., **55**, No. 5, 534 – 543 (2019).
12. *L.V. Mol'chenko, I.I. Loos and V.N. Darmosyuk.* "Thermomagnetoelastic deformation of flexible orthotropic shells of revolution of variable stiffness with Joule heat taken into account," Int. Appl. Mech., **56**, No. 4, 498 – 511 (2020).
13. *L.V. Mol'chenko and I.I. Loos* "Magnetoelastic deformation of flexible orthotropic ring plate with orthotropic conductivity and Joule heat," Int. Appl. Mech., **57**, No. 2, 217 – 233 (2021).
14. *Y.H. Bian.* "Analysis of nonlinear stresses and strains in a thin current-carrying elastic plate," Int. Appl. Mech., **51**, No. 1, 108 – 120 (2015).
15. *Y.H. Bian and Q. You.* "Analysis of thermal-magnetic-elastic stresses and strains in a thin annular plate with varying thickness," Int. Appl. Mech., **57**, No. 1, 111 – 121 (2021).
16. *X.J. Zheng and X.Z. Wang.* "A magnetoelastic theoretical model for soft ferromagnetic shell in magnetic field," Int. J. Solids Struct., **40**, No. 24, 6897 – 6912 (2003).
17. *D.J. Hasanyan, L.Librescu and D.R. Ambur.* "Buckling and postbuckling of magnetoelastic flat plates carrying an electric current," Int. J. Solids Struct., **43**, No. 16, 4971 – 4996 (2006).
18. *Y.W. Gao and B. Xu.* "Dynamic behaviors of conductive circular plate in time-varying magnetic fields," Acta Mechanica Solida Sinica, **23**, No. 1, 66 – 76 (2010).
19. *Z.B. Kuang.* "An applied electro-magneto-elastic thin plate theory," Acta Mechanica, **225**, No. 4, 1153 – 1166 (2014).
20. *M. Vinyas, P.J. Sagar and S. Kattimani.* "Influence of coupled fields on free vibration and static behavior of functionally graded magneto-electro-thermo-elastic plate," J. of Intelligent Material Systems and Structures, **29**, No. 7, 1430 – 1455 (2018).
21. *H.H. Bi, B. Wang, Z.C. Deng and S.D. Wang.* "Effects of thermo-magneto-electro nonlinearity characteristics on the stability of functionally graded piezoelectric beam," Applied Mathematics and Mechanics, **41**, No. 2, 313 – 326 (2020).
22. *M.A. Mihaeev*. Basis of Heat Transfer [in Chinese], High Education Press, Beijing (1958).

From the Editorial Board: The article corresponds completely to submitted manuscript.

Надійшла 09.09.2021 Затверджена до друку 28.03.2023